Physics Letters B 823 (2021) 136766

Contents lists available at ScienceDirect

Physics Letters B

www.elsevier.com/locate/physletb

Impact of shell evolution on Gamow-Teller β decay from a high-spin long-lived isomer in ^{127}Ag

H. Watanabe [a,b,*], C.X. Yuan [c], G. Lorusso [b,d,e], S. Nishimura [b], Z.Y. Xu [f], T. Sumikama [g,b], P.-A. Söderström [b,h], P. Doornenbal [b], F. Browne [b,i], G. Gey [b,j], H.S. Jung [k], J. Taprogge [b,l,m], Zs. Vajta [b,n], H.K. Wang [o], J. Wu [b,p,q], A. Yagi [r], H. Baba [b], G. Benzoni [s], K.Y. Chae [t], F.C.L. Crespi [s,u], N. Fukuda [b], R. Gernhäuser [v], N. Inabe [b], T. Isobe [b], A. Jungclaus [m], D. Kameda [b], G.D. Kim [w], Y.K. Kim [w,x], I. Kojouharov [y], F.G. Kondev [q], T. Kubo [b], N. Kurz [y], Y.K. Kwon [w], G.J. Lane [z], Z. Li [p], C.-B. Moon [aa], A. Montaner-Pizá [ab], K. Moschner [ac], F. Naqvi [ad], M. Niikura [f], H. Nishibata [r], D. Nishimura [ae], A. Odahara [r], R. Orlandi [af], Z. Patel [e], Zs. Podolyák [e], H. Sakurai [b], H. Schaffner [y], G.S. Simpson [j], K. Steiger [v], H. Suzuki [b], H. Takeda [b], A. Wendt [ac], K. Yoshinaga [ag]

[a] *School of Physics, and International Research Cernter for Nuclei and Particles in Cosmos, Beihang University, Beijing 100191, China*
[b] *RIKEN Nishina Center, 2-1 Hirosawa, Wako, Saitama 351-0198, Japan*
[c] *Sino-French Institute of Nuclear Engineering and Technology, Sun Yat-Sen University, Zhuhai, 519082, Guangdong, China*
[d] *National Physical Laboratory, NPL, Teddington, Middlesex TW11 0LW, United Kingdom*
[e] *Department of Physics, University of Surrey, Guildford GU2 7XH, United Kingdom*
[f] *Department of Physics, University of Tokyo, Hongo, Bunkyo-ku, Tokyo 113-0033, Japan*
[g] *Department of Physics, Tohoku University, Aoba, Sendai, Miyagi 980-8578, Japan*
[h] *Extreme Light Infrastructure-Nuclear Physics (ELI-NP)/Horia Hulubei National Institute for Physics and Nuclear Engineering (IFIN-HH), Str. Reactorului 30, 077125 Bucharest-Măgurele, Romania*
[i] *School of Computing, Engineering and Mathematics, University of Brighton, Brighton, BN2 4GJ, United Kingdom*
[j] *LPSC, Université Joseph Fourier Grenoble 1, CNRS/IN2P3, Institut National Polytechnique de Grenoble, F-38026 Grenoble Cedex, France*
[k] *Department of Physics, Chung-Ang University, Seoul 156-756, Republic of Korea*
[l] *Departamento de Física Teórica, Universidad Autónoma de Madrid, E-28049 Madrid, Spain*
[m] *Instituto de Estructura de la Materia, CSIC, E-28006 Madrid, Spain*
[n] *MTA Atomki, P. O. Box 51, Debrecen, H-4001, Hungary*
[o] *College of Physics and Telecommunication Engineering, Zhoukou Normal University, Henan 466000, China*
[p] *School of Physics and State Key Laboratory of Nuclear Physics and Technology, Peking University, Beijing 100871, China*
[q] *Physics Division, Argonne National Laboratory, Argonne, IL 60439, USA*
[r] *Department of Physics, Osaka University, Machikaneyama-machi 1-1, Osaka 560-0043 Toyonaka, Japan*
[s] *INFN, Sezione di Milano, via Celoria 16, I-20133 Milano, Italy*
[t] *Department of Physics, Sungkyunkwan University, Suwon 440-746, Republic of Korea*
[u] *Dipartimento di Fisica, Universitá di Milano, via Celoria 16, I-20133 Milano, Italy*
[v] *Physik Department, Technische Universität München, D-85748 Garching, Germany*
[w] *Rare Isotope Science Project, Institute for Basic Science, Daejeon 305-811, Republic of Korea*
[x] *Department of Nuclear Engineering, Hanyang University, Seoul 133-791, Republic of Korea*
[y] *GSI Helmholtzzentrum für Schwerionenforschung GmbH, 64291 Darmstadt, Germany*
[z] *Department of Nuclear Physics, R.S.P.E., Australian National University, Canberra, A.C.T 2601, Australia*
[aa] *Department of Display Engineering, Hoseo University, Chung-Nam 336-795, Republic of Korea*
[ab] *IFIC, CSIC-Universidad de Valencia, A.C. 22085, E 46071, Valencia, Spain*
[ac] *Institut für Kernphysik, Universität zu Köln, Zülpicher Strasse 77, D-50937 Köln, Germany*
[ad] *Wright Nuclear Structure Laboratory, Yale University, New Haven, CT 06520-8120, USA*
[ae] *Department of Physics, Tokyo City University, Setagaya-ku, Tokyo 158-8557, Japan*
[af] *Instituut voor Kern en Stralingsfysica, KU Leuven, University of Leuven, B-3001 Leuven, Belgium*
[ag] *Department of Physics, Faculty of Science and Technology, Tokyo University of Science, 2641 Yamazaki, Noda, Chiba, Japan*

* Corresponding author at: School of Physics, and International Research Cernter for Nuclei and Particles in Cosmos, Beihang University, Beijing 100191, China.
E-mail address: hiroshi@ribf.riken.jp (H. Watanabe).

https://doi.org/10.1016/j.physletb.2021.136766

ARTICLE INFO

Article history:
Received 30 July 2021
Received in revised form 27 October 2021
Accepted 1 November 2021
Available online 4 November 2021
Editor: D.F. Geesaman

Keywords:
Shell evolution
Gamow-Teller β decay
Isomer
^{127}Ag
Radioactive isotope beam

ABSTRACT

The change of the shell structure in atomic nuclei, so-called "*nuclear shell evolution*", occurs due to changes of major configurations through particle-hole excitations inside one nucleus, as well as due to variation of the number of constituent protons or neutrons. We have investigated how the shell evolution affects Gamow-Teller (GT) transitions that dominate the β decay in the region below ^{132}Sn using the newly obtained experimental data on a long-lived isomer in ^{127}Ag. The $T_{1/2} = 67.5(9)$ ms isomer has been identified with a spin and parity of $(27/2^+)$ at an excitation energy of 1942^{+14}_{-20} keV, and found to decay via an internal transition of an $E3$ character, which competes with the dominant β-decay branches towards the high-spin states in ^{127}Cd. The underlying mechanism of a strong GT transition from the ^{127}Ag isomer is discussed in terms of configuration-dependent optimization of the effective single-particle energies in the framework of a shell-model approach.

The decay properties of unstable nuclei reflect the underlying nuclear-structure aspects such as single-particle and collective degrees of freedom, which interplay with each other and thereby give rise to a rich variety of phenomena, *e.g.*, shape coexistence [1,2], neutron halo/skin structures [3,4], and nuclear isomers [5,6]. From astrophysical point of view, a breadth of knowledge on radioactive-decay processes is required for a better description of nucleosynthesis under (explosive) stellar environments [7]. In the rapid-neutron capture (r) process [8], for instance, the β-decay properties of neutron-rich isotopes far from stability play an important role in forming the abundance pattern, in particular, the three prominent peaks around mass numbers $A = 80$, 130, and 195, which are fingerprints stemming from the shell closures at neutron numbers $N = 50$, 82, and 126, respectively [9]. Thus, understanding the radioactive decays and associated nuclear structure is one of the key factors that will lead to a comprehensive understanding of the question of how the elements from iron to uranium are created in the universe.

New results in the field of nuclear physics obtained in the last two decades [10] include new or lost magic numbers in some regions of exotic nuclei with an extremely unbalanced ratio of protons and neutrons [11]. This novel phenomenon emerges as a result of change of single-particle energies (SPEs), or alternatively called *shell evolution*, in which the monopole component of the nucleon-nucleon interaction plays a pivotal role [12,13]. It is widely known nowadays that the shell structure varies with the proton or neutron number, whereas the other important cause of shell evolution, being due to particle-hole excitations in exotic nuclei [14], remains poorly understood. In this Letter, we focus on the effect of shell evolution on Gamow-Teller (GT) transitions, which dominate the β decay in the south-west region of the doubly magic nucleus ^{132}Sn. The experimental probe is a previously unreported high-spin isomer in ^{127}Ag (proton number $Z = 47$ and $N = 80$), which enables an exploration of the daughter levels at high spins that are normally inaccessible by other means.

The present work has been conducted at Radioactive Isotope Beam Factory (RIBF) [15] as part of the EURICA project [16]. A radioactive isotope beam of ^{127}Ag was separated/identified through the fragment separator BigRIPS [17], following its production via in-flight fission of a 345-MeV/u $^{238}U^{86+}$ beam incident on a 3-mm thick Be target. With an average beam intensity of 10 pnA, about 1.5 million ^{127}Ag fragments were implanted into the WAS3ABi active stopper [16] that consisted of eight $60 \times 40 \times 1$ mm double-sided silicon-strip detectors (DSSSDs) stacked compactly. The DSSSDs also served to detect β rays and internal conversion (IC) electrons emitted subsequently from the implanted ions. Gamma rays were detected by 12 Cluster-type high-purity Ge detectors [18].

In ^{127}Cd, the β-decay daughter of ^{127}Ag, an isomeric state with $T_{1/2} = 17.5(3)$ μs and $J^\pi = (19/2^+)$ was previously identified at 1560 keV relative to the $11/2^-$ state [19]. In the present work, the 739- and 821-keV γ rays, which were assigned as forming the $(19/2^+) \rightarrow (15/2^-) \rightarrow 11/2^-$ cascade in ^{127}Cd [19], have been unambiguously observed following the ^{127}Ag implantation, as exhibited in Fig. 1(a). It is unlikely that such high-spin states are populated in the β decay from the ground state of ^{127}Ag, which is supposed to have $J^\pi = 9/2^+$ from the level systematics for the lighter odd-A Ag isotopes [20]. Therefore, this observation is a clear indication that there is a β-decaying isomer at high spin in ^{127}Ag (hereinafter denoted as ^{127m}Ag).

The level scheme of ^{127}Cd populated in the β decay from ^{127m}Ag is depicted in Fig. 2 (lower), where the excitation energies are calculated relative to the $11/2^-$ state, which was identified as a long-lived isomer, along with the $3/2^+$ ground state, from recent mass measurements [21,22]. The placement of transitions above the 1560-keV state is based on their (prompt) coincidence relationships, as demonstrated in Figs. 1(b) and 1(c). The half-life of the $(19/2^+)$ isomer derived from a γ-γ time difference [see Fig. 3(a)] is in good agreement with the previously reported value [19]. Furthermore, a fit to the time difference between the 242- and 306-keV γ rays yields $T_{1/2} = 8.9(5)$ ns [Fig. 3(b)]. Since the reduced transition probability for $E_\gamma = 242$ keV, $B(E2) = 1.9(1)$ W.u., is comparable to the corresponding $23/2^+ \rightarrow 19/2^+$ transitions in the $N = 79$ isotones ^{129}Sn [23] and ^{125}Pd [24], the 8.9-ns isomer in ^{127}Cd is assigned $J^\pi = (23/2^+)$. The β-branching ratio I_β to each excited state was derived from the intensity balance between the incoming and outgoing transitions, taking into account the efficiency-corrected γ-ray intensities that are summarized in Table 1 and theoretical total conversion coefficients for possible multipolarities. It should be noted that the I_β values evaluated here are considered as upper limits, due to possible unobserved feedings from higher-lying states [25]. (Such unobserved γ rays, whose relative intensity is expected to be 1% or less, if any, will not cause a serious change in the deduced I_β.) Since there is no apparent β feeding ($I_\beta \approx 0$) to the $J^\pi = (23/2^+)$ state in ^{127}Cd, the spin of ^{127m}Ag is expected to be 27/2 or higher.

For ^{127}Ag, nothing is known so far about its excited level structure. In Fig. 1(d), six γ-ray peaks become prominent when gating on electrons at low energy in DSSSD, where IC electrons are predominant over β rays in case there exists a long-lived isomer that undergoes internal transition (IT) [28–31]. Therefore, these γ rays are expected to follow the IT decay from ^{127m}Ag. The 687-keV transition is assigned as $(13/2^+) \rightarrow (9/2^+)$ based on its intensity and the systematics for the lighter odd-A Ag isotopes [32,20]. In Figs. 3(c)-3(e), the 687-keV γ ray exhibits a similar time behavior to the 739- and 242-keV transitions of ^{127}Cd, suggesting that they originated from one isomeric state. A weighted average of the re-

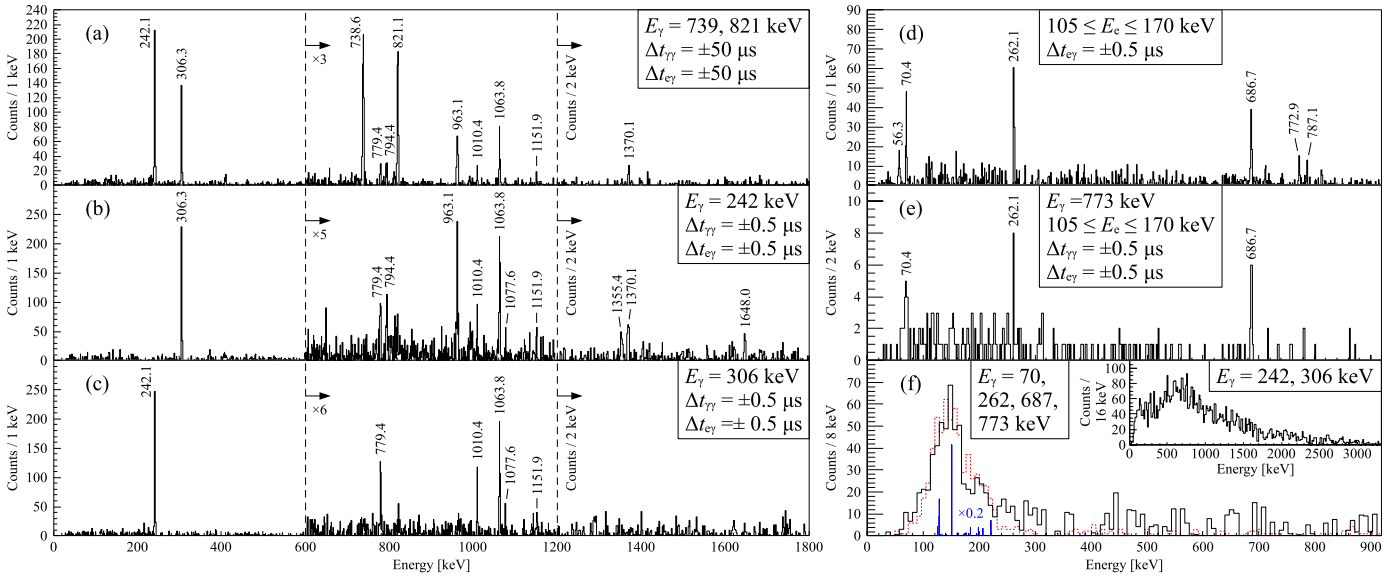

Fig. 1. Energy spectra of γ rays (a)-(e) and electrons (f) measured within 100 ms after implantation of ^{127}Ag ions with coincidence gates as indicated in squares. In the panel (f), the dashed red and solid blue lines represent the results of Monte Carlo simulations with and without consideration for the detector resolution, respectively, for $E_{IT} = 150$ keV.

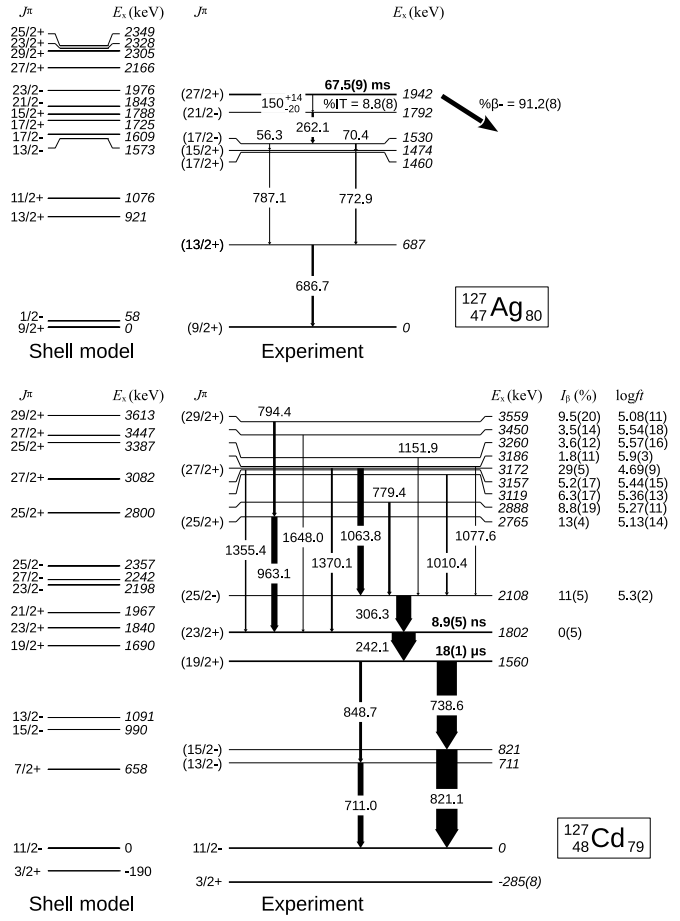

Fig. 2. Experimental and theoretical level schemes of ^{127}Ag and ^{127}Cd. The widths of vertical arrows are proportional to the γ-ray intensities summarized in Table 1. $Q_\beta = 10090(200)$ keV [26] and $E_x = -285(8)$ keV for the $J^\pi = 3/2^+$ level in ^{127}Cd [27] are taken into account in the calculation of logft. Spins and parities in parentheses represent tentative ones.

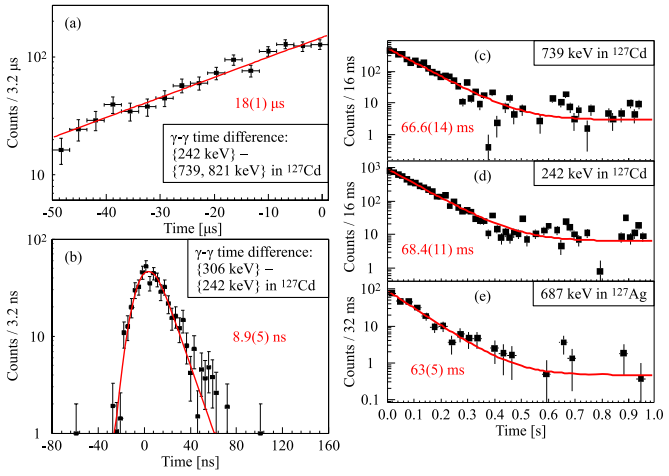

Fig. 3. Decay curves and associated fits for γ-γ time differences (a)-(b) and γ rays relative to implantation of ^{127}Ag ions (c)-(e).

spective fits to the decay curves results in $T_{1/2} = 67.5(9)$ ms for ^{127m}Ag. It should be noted that the measured isomeric half-life is somewhat shorter than 89(2) ms, the value reported previously on ^{127}Ag [33], which should mainly reflect the ground-state half-life. The IT/β-branching ratios are determined to be 8.8(8)/91.2(8) % from the total intensities of the 687-keV (^{127}Ag) and 242-keV (^{127}Cd) transitions.

The IT-decay scheme from ^{127m}Ag is proposed as displayed in Fig. 2 (upper). It was found by a γ-γ coincidence analysis [see Fig. 1(e)] that two parallel cascades via 56 – 787 and 70 – 773 keV intervene between the 687- and 262-keV transitions. The levels at 1460 and 1474 keV were tentatively assigned $(17/2^+)$ and $(15/2^+)$, respectively, which are interpreted as a proton in the $g_{9/2}$ orbital coupled to the 4_1^+ state at 1481 keV in the neighboring $N = 80$ isotone ^{126}Pd [34]. The total conversion coefficients α_T of the 56- and 70-keV transitions were evaluated to be smaller than 0.7 and 0.2 (within one standard deviation) from the intensity balance analysis for the respective cascades. Such small α_T values are

Table 1
Summary of transitions in ^{127}Cd and ^{127}Ag populated in the decay from ^{127m}Ag.

Nucleus	E_γ (keV)	I_γ(%)[a]	Initial state		Final state	
			E_x (keV)[b]	J^π	E_x (keV)[b]	J^π
^{127}Cd	242.1	100	1801.8	$(23/2^+)$	1559.7	$(19/2^+)$
	306.3	63(3)	2108.1	$(25/2^-)$	1801.8	$(23/2^+)$
	711.0	24(3)	711.0	$(13/2^-)$	0.0	$11/2^-$
	738.6	84(4)	1559.7	$(19/2^+)$	821.1	$(15/2^-)$
	779.4	10(2)	2887.5		2108.1	$(25/2^-)$
	794.4	11(2)	3559.3	$(29/2^+)$	2765	$(25/2^+)$
	821.1	89(4)	821.1	$(15/2^-)$	0.0	$(11/2^-)$
	848.7	12(2)	1559.7	$(19/2^+)$	711.0	$(13/2^-)$
	963.1	26(4)	2764.9	$(25/2^+)$	1801.8	$(23/2^+)$
	1010.4	7.3(18)	3118.5		2108.1	$(25/2^-)$
	1063.8	27(4)	3171.9	$(27/2^+)$	2108.1	$(25/2^-)$
	1077.6	2.1(12)	3185.7		2108.1	$(25/2^-)$
	1151.9	4.2(13)	3260.0		2108.1	$(25/2^-)$
	1355.4	6.1(18)	3157.2		1801.8	$(23/2^+)$
	1370.1	7.5(20)	3171.9	$(27/2^+)$	1801.8	$(23/2^+)$
	1648.0	4.1(15)	3449.8		1801.8	$(23/2^+)$
^{127}Ag	56.3	3.3(12)	1530.0	$(17/2^-)$	1473.7	$(15/2^+)$
	70.4	6.6(12)	1530.0	$(17/2^-)$	1459.6	$(17/2^+)$
	150^{+14}_{-20}	$3.3^{+1.4}_{-1.5}$[c]	1942^{+14}_{-20}	$(27/2^+)$	1792.1	$(21/2^-)$
	262.1	10.1(12)	1792.1	$(21/2^-)$	1530.0	$(17/2^-)$
	686.7	10.3(10)	686.7	$(13/2^+)$	0.0	$(9/2^+)$
	772.9	6.4(8)	1459.6	$(17/2^+)$	686.7	$(13/2^+)$
	787.1	3.9(6)	1473.7	$(15/2^+)$	686.7	$(13/2^+)$

[a] Relative to the intensity of the 242-keV γ ray in ^{127}Cd.
[b] Relative energy from the $11/2^-$ state in ^{127}Cd (upper) and from the $(9/2^+)$ state in ^{127}Ag (lower).
[c] Estimated from the balance of the total transition intensity $(1+\alpha_T)I_\gamma$ with the 262-keV transition in ^{127}Ag.

indicative of $E1$ character, whereby the 1530-keV state is assigned $(17/2^-)$. Similarly, the value obtained for the 262-keV transition, $\alpha_T = 0.02(15)$, is consistent with dipole and quadrupole multipolarities within the margin of error. As the 1792-keV state decays only to the $(17/2^-)$ level, but neither to the lower-lying $(15/2^+)$ nor $(17/2^+)$ levels, $J^\pi = (21/2^-)$ is assigned for this level.

In the electron energy (E_e) spectra shown in Fig. 1(f), a bunch of events emerge at $E_e \lesssim 250$ keV with a sum of gates on the IT γ rays. They are ascribed mainly to the IC (and the following atomic) processes for the transition(s) de-exciting ^{127m}Ag. Note that the emission of γ ray that competes with the IC process can not be viewed in Fig. 1(d) by gating on $E_e = 105 - 170$ keV. To estimate the de-excitation energy in the IT-decay branch ($E_{\rm IT}$), we have conducted Monte Carlo simulations using the GEANT4 toolkit [35] by taking into account the observed decay schemes (Fig. 2) with the assumption that ^{127m}Ag decays via a single $E3$ transition. The observed IT-γ gated E_e spectrum was fitted to a detector response function, which was determined by the simulation performed for a given value of $E_{\rm IT}$ with an energy resolution of 50 keV (FWHM) for the DSSSDs. The χ^2 analysis resulted in $E_{\rm IT} = 150^{+14}_{-20}$ keV with the 1σ confidence interval, for which the $B(E3)$ value is evaluated to range from 0.2 to 0.49 W.u., comparable to those observed in this region (see Table 2 in Ref. [36]). Based on these arguments, ^{127m}Ag is assigned $J^\pi = (27/2^+)$ at $E_x = 1942^{+14}_{-20}$ keV.

As can be seen in Fig. 2, the state at 3172 keV in ^{127}Cd is most strongly populated with $\log ft$ = 4.69(9), obviously indicating the occurrence of an allowed GT transition. This value is close to $\log ft$ = 4.4 derived for the β decay from the $9/2^+$ ground state in ^{131}In to the first $7/2^+$ state in ^{131}Sn [37], which also proceeds predominantly with the GT transition. (For the ^{131}In $\rightarrow$ ^{131}Sn GT transition, a comparison with a shell-model calculation is presented in Ref. [38].) The β feedings towards the 3559- and 2765-keV states are found to have $\log ft = 5.08(11)$ and 5.13(14), respectively, which are comparable to those derived from the decays in the lighter Ag isotopes, ^{124,126}Ag $(8^-) \rightarrow$ ^{124,126}Cd (7^-) [39] and ^{123}Ag $(7/2^+) \rightarrow$ ^{123}Cd $(5/2^+)$ [40]. Thus, the 3559- and 2765-keV states of ^{127}Cd are also interpreted as being populated via allowed transitions. In conjunction with the observed feeding patterns towards the lower-lying levels, the 3559-, 3172-, and 2765-keV states are assigned $(29/2^+)$, $(27/2^+)$, and $(25/2^+)$, respectively.

With the aim of understanding the observed level structure and GT transitions, we performed shell-model calculations in the same framework as our previous study on ^{123}Ag and ^{125}Ag [20]: The model space considered includes four orbitals in the $Z = 28 - 50$ major shell for protons and five orbitals in the $N = 50 - 82$ major shell for neutrons above the inert core ^{78}Ni, and the effective nucleon-nucleon interaction arises from the monopole-based universal interaction $V_{\rm MU}$ [12] plus a spin-orbit force taken from the M3Y interaction [41]. The $V_{\rm MU}$ interaction, which consists of the finite-range central force and the spin-isospin dependent tensor force, was applied successfully to other nuclei [42–44]. Being different from the previous study [20], there is no constraint on the orbital occupancy within the model space in the present calculations. As compared in Fig. 2, both for ^{127}Ag and ^{127}Cd, the shell-model calculations provide an adequate description of the observed level structure up to $J = 29/2$. The lowest $27/2^+$ state in ^{127}Ag is predicted to be a long-lived isomer, which decays via an $M2$ transition or/and an $E3$ transition, the latter being consistent with what was observed experimentally.

In the $Z < 50$ and $N \leq 82$ region, β decay proceeds mainly with GT transitions that involve the transformation of a neutron (ν) in the $g_{7/2}$ orbital to a proton (π) in the $g_{9/2}$ orbital. Thus, the GT transition strength B(GT) is sensitive to the occupancy of $\nu g_{7/2}$ and the vacancy of $\pi g_{9/2}$. The measured and calculated B(GT) values are summarized in Table 2. For the GT transitions from the $27/2^+$ state in ^{127}Ag to the $25/2^+$, $27/2^+$, and $29/2^+$ states in ^{127}Cd, the B(GT) values obtained in the present calculation compare well with the respective experimental values. Here, all the theoretical B(GT) values were calculated using a quenching factor of 0.6, which was adopted so that the predicted half-lives of the ground and isomeric states of ^{127}Ag are comparable to the observed values. The quenching of B(GT) is considered to arise from

Table 2
B(GT) values from the $27/2^+$ state of ^{127}Ag. The experimental B(GT) values are evaluated as $B(\mathrm{GT})^{\mathrm{ex}} = \frac{6147}{ft(g_A/g_V)^2}$ with $g_A/g_V = -1.266$ [49], while all the shell-model $B(\mathrm{GT})^{\mathrm{th}}$ values are multiplied by the square of a quenching factor of 0.6.

Transition	$B(\mathrm{GT})^{\mathrm{ex}}$	$B(\mathrm{GT})^{\mathrm{th}}$
^{127}Ag$(27/2^+) \rightarrow {}^{127}Cd(27/2^+)$	0.078(16)	0.088
^{127}Ag$(27/2^+) \rightarrow {}^{127}Cd(29/2^+)$	0.032(8)	0.024
^{127}Ag$(27/2^+) \rightarrow {}^{127}Cd(25/2^+)$	0.028(9)	0.014

lacking many-body correlations and neglected contributions from meson-exchange currents in nuclear models [45]. The first effect is ascribed predominantly to the insufficient single-particle description of the nuclear level. In the present shell-model calculation, as the proton orbitals above $Z = 50$ and the neutron orbitals below $N = 50$ are not included explicitly in the model space, some of the proton particle-neutron hole matrix elements of a one-body GT operator, such as the $\pi g_{7/2}$-$\nu g_{7/2}^{-1}$ and $\pi g_{7/2}$-$\nu g_{9/2}^{-1}$ pairs, are missing. The inadequacy of such first-order components in the model space may be a possible cause of the slightly smaller quenching factor adopted in the current calculation than in the previous shell-model works [38,46,47]. However, further discussion about the origin of the quenching phenomenon is beyond the scope of this article, and a calculation of B(GT) for the $27/2^+$ isomeric decay with an extended model space remains a challenge for future theoretical works.

To gain a further insight into the underlying mechanism of the GT β decay from $^{127\mathrm{m}}$Ag, the shell-model wave functions of the parent and daughter $27/2^+$ states are analyzed: The configuration of the $27/2^+$ state in ^{127}Ag is dominated by the $\pi(g_{9/2}^{-3}) \otimes \nu(h_{11/2}^{-2})$ component with an amplitude of 80%. This dominant component can give rise to $27/2^+$ through the coupling of the $\pi(g_{9/2}^{-3})_{7/2^+}$ excitation to the $\nu(h_{11/2}^{-2})_{10^+}$ state, which was identified previously as a long-lived (10^+) isomer in the neighboring $N = 80$ isotone ^{126}Pd [28]. Concerning the $27/2^+$ state in the daughter nucleus ^{127}Cd, the probability of the $\pi(g_{9/2}^{-2}) \otimes \nu(g_{7/2}^{-1}h_{11/2}^{-2})$ component is 66%, thereby yielding a sizable B(GT) value from the parent $27/2^+$ state via the $\nu g_{7/2} \rightarrow \pi g_{9/2}$ transition. With this leading component, a spin and parity of $27/2^+$ is generated as a result of a fully aligned coupling of one $g_{7/2}$ and two $h_{11/2}$ neutron holes (together with an inactive proton-hole pair coupled to spin zero).

In the present shell-model calculation, the effective SPEs (ESPEs) are computed on a configuration-by-configuration basis. When an orbital j_b is filled, the shift of ESPE of an orbital j_a, $\Delta\epsilon_{j_a}$, depends on the expectation value of the occupation number n_{j_b} [48]; $\Delta\epsilon_{j_a} = v_{m,j_aj_b} n_{j_b}$, where v_{m,j_aj_b} represents the monopole component of a given two-body interaction between the nucleons in j_a and j_b. Thus, the ESPE optimization occurs differently for each (excited) state due to different occupation patterns and the orbital dependences of the monopole interaction. Figs. 4(a)/4(b) exhibit the proton/neutron ESPEs and their respective occupation numbers expected for the $9/2^+$ and $27/2^+$ states in ^{127}Ag and for the $11/2^-$ and $27/2^+$ states in ^{127}Cd. The proton and neutron SPEs shown in the middle column in Fig. 4 correspond to the excitation energies of the empirical single-hole states in ^{131}In and ^{131}Sn, respectively.

Comparing the ESPEs at the $11/2^-$ and $27/2^+$ states in ^{127}Cd [see the fourth and fifth columns in Figs. 4(a) and 4(b)], one can notice two important aspects: Firstly, the energy spacing between the $\pi g_{9/2}$ and $\pi p_{1/2}$ orbitals, which defines the $Z = 40$ subshell gap [20], increases by a factor of 3 or more along with the excitation from $11/2^-$ to $27/2^+$. As such an enlargement of the energy gap tends to hamper the cross-shell excitation, the $\pi(g_{9/2}^{-2})$ coupling is energetically favored in the two proton-hole nucleus. Secondly, the order of the $\nu g_{7/2}$ and $\nu d_{5/2}$ orbitals is inverted. A similar level inversion is also found for the $\nu h_{11/2}$ and $\nu d_{3/2}$ orbitals. Due to these modifications in the neutron ESPEs, the $\nu(g_{7/2}^{-1}h_{11/2}^{-2})$ coupling is allowed to manifest itself at rather low energy in the three neutron-hole system. Thus, both the proton and neutron ESPEs are optimized so that the lowest $27/2^+$ state of ^{127}Cd has a large proportion of the $\pi(g_{9/2}^{-2}) \otimes \nu(g_{7/2}^{-1}h_{11/2}^{-2})$ configuration. Compared to the $11/2^- \Rightarrow 27/2^+$ excitation in ^{127}Cd, the inversion of the $\nu g_{7/2}$ and $\nu d_{5/2}$ orbitals is predicted to happen more steeply for the $9/2^+ \Rightarrow 27/2^+$ excitation in ^{127}Ag, as illustrated from the second to first column in Fig. 4(b). The upward drift of $\nu g_{7/2}$ approaching the Fermi surface enables to facilitate the removal of a neutron from that orbital. Therefore, for both the parent and daughter nuclei, the ESPE optimization takes place in order to enhance a GT β decay between the high-spin states. Such configuration-dependent optimization mechanism, called "self-organization [42]", is suggested to play a crucial role in various aspects of atomic nuclei consisting of protons and neutrons.

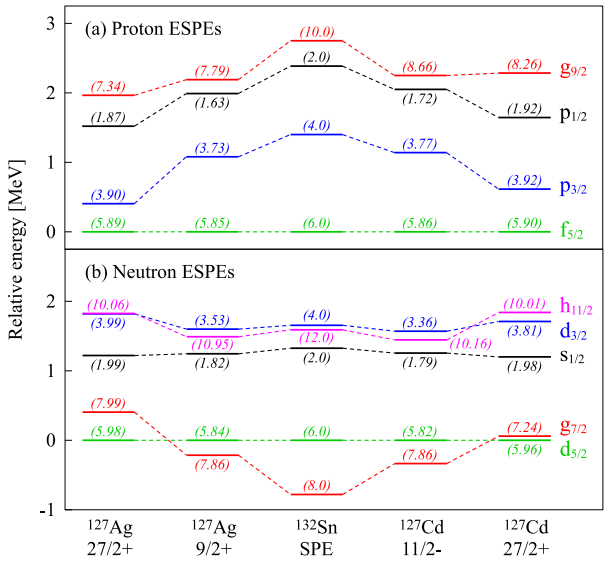

Fig. 4. Effective single-particle energies (ESPEs) of proton (a) and neutron (b) at the $11/2^-$ and $27/2^+$ states in ^{127}Cd and the $9/2^+$ and $27/2^+$ states in ^{127}Ag given in the current shell-model calculation. In the central column, the SPEs in ^{132}Sn are exhibited for reference. Numbers in parentheses represent the occupation number. The dashed lines connecting the same shell orbitals are a guide to the eye.

The most notable feature in the ESPE plots shown in Fig. 4 is that the $\nu g_{7/2}$ orbital rises quickly not only when the system moves away from the doubly magic nucleus ^{132}Sn, but also when changing major configurations within the same nucleus. The main cause of this orbital shift is a decrease in the occupancy of the $\pi g_{9/2}$ orbital, which leads to a loss of an attractive monopole interaction that works strongly between the spin-orbit pair, $\pi g_{9/2}$ and $\nu g_{7/2}$. The shell evolution due to varying proton or neutron number is called Type I shell evolution [14], and its effect on the β-decay properties of the r-process nuclei around $N = 82$ was discussed in Refs. [38,47]. In contrast to the more conventional Type I shell evolution, the present study on the high-spin isomer in ^{127}Ag indicates that a combined effect of the proton-neutron monopole interaction and changes of major configurations (referred to as Type II shell evolution [14]) is significant for developing a GT β decay from (long-lived) excited states that involve specific particle-hole excitations.

In summary, a previously unreported isomer with a half-life of 67.5(9) ms has been identified at an excitation energy of 1942^{+14}_{-20} keV in ^{127}Ag. This isomeric state was tentatively assigned $(27/2^+)$, and found to undergo an internal $E3$ decay and external β decay with a strong Gamow-Teller (GT) transition towards the $(27/2^+)$

state in the daughter nucleus ^{127}Cd. The observed level energies and GT transition strengths were well reproduced by the shell-model calculations, in which the effective single-particle energies (ESPEs) are calculated on a configuration-by-configuration basis. In comparison with the shell model, we shed light on the effect of shell evolution, which occurs not only with variation of proton or neutron number, but also with changes of major configurations inside one nucleus. It turned out that the shell evolution (*i.e.*, ESPE optimization) takes place so that the GT transition between high-spin states is enhanced. Such configuration-dependent optimization of the ESPEs plays an important role in determining the β-decay properties of very neutron-rich nuclides in this region relevant to the *r*-process nucleosynthesis.

We thank the staff at RIBF for providing the beams, the EUROBALL Owners Committee for the loan of germanium detectors, the PreSpec Collaboration for the use of the readout electronics. Part of the WAS3ABi was supported by the Rare Isotope Science Project which is funded by MSIP and NRF of Korea. This work was supported by the Priority Centers Research Program in Korea (2009-0093817), OTKA contract number K100835, the U.S. DOE, Office of Nuclear Physics (Contract No. DE-AC02-06CH11357), NRF-2016R1A5A1013277 and NRF-2013M7A1A1075764, the Spanish Ministerio de Economía y Competitividad under contract FPA2017-84756-C4-2-P, the European Commission through the Marie Curie Actions call FP7-PEOPLE-2011-IEF (Contract No. 300096), German BMBF under Contract No: 05P12PKFNE, JSPS KAKENHI Grant No. 24740188 and 25247045, the National Natural Science Foundation of China (Nos. 11505302, 11575112, 11775316), the National Key Program for S&T Research and Development (No. 2016YFA0400501), and STFC (UK).

Declaration of competing interest

The authors declare that they have no known competing financial interests or personal relationships that could have appeared to influence the work reported in this paper.

References

[1] K. Heyde, et al., Rev. Mod. Phys. 83 (2011) 1467.
[2] J.L. Wood, et al., J. Phys. G, Nucl. Part. Phys. 43 (2016) 020402.
[3] I. Tanihata, et al., Phys. Rev. Lett. 55 (1985) 2676.
[4] P.G. Hansen, et al., Europhys. Lett. 4 (1987) 409.
[5] P. Walker, et al., Nature 399 (1999) 35.
[6] G.D. Dracoulis, et al., Rep. Prog. Phys. 79 (2016) 076301.
[7] R. Diehl, Astrophysics with Radioactive Isotopes, Springer International Publishing, Cham, 2018, pp. 3–27.
[8] E.M. Burbidge, et al., Rev. Mod. Phys. 29 (1957) 547.
[9] T. Kajino, et al., Prog. Part. Nucl. Phys. 107 (2019) 109.
[10] T. Nakamura, et al., Prog. Part. Nucl. Phys. 97 (2017) 53.
[11] O. Sorlin, et al., Prog. Part. Nucl. Phys. 61 (2008) 602.
[12] T. Otsuka, et al., Phys. Rev. Lett. 104 (2010) 012501.
[13] T. Otsuka, et al., Rev. Mod. Phys. 92 (2020) 015002.
[14] T. Otsuka, et al., J. Phys. G, Nucl. Part. Phys. 43 (2016) 024009.
[15] Y. Yano, Nucl. Instrum. Methods Phys. Res. B 261 (2007) 1009.
[16] S. Nishimura, Prog. Theor. Exp. Phys. 2012 (2012) 03C006.
[17] T. Kubo, et al., Prog. Theor. Exp. Phys. 2012 (2012) 03C003.
[18] P.-A. Söderström, et al., Nucl. Instrum. Methods Phys. Res. B 317 (2013) 649.
[19] F. Naqvi, et al., Phys. Rev. C 82 (2010) 034323.
[20] Z.Q. Chen, et al., Phys. Rev. Lett. 122 (2019) 212502.
[21] D. Lascar, et al., Phys. Rev. C 96 (2017) 044323.
[22] V. Manea, et al., Phys. Rev. Lett. 124 (2020) 092502.
[23] J. Genevey, et al., Phys. Rev. C 65 (2002) 034322.
[24] H. Watanabe, et al., Phys. Lett. B 792 (2019) 263.
[25] J. Hardy, et al., Phys. Lett. B 71 (1977) 307.
[26] W. Huang, et al., Chin. Phys. C 45 (2021) 030002.
[27] F. Kondev, et al., Chin. Phys. C 45 (2021) 030001.
[28] H. Watanabe, et al., Phys. Rev. Lett. 113 (2014) 042502.
[29] J. Taprogge, et al., Phys. Lett. B 738 (2014) 223.
[30] H. Watanabe, et al., Phys. Lett. B 760 (2016) 641.
[31] J.J. Liu, et al., Phys. Rev. C 102 (2020) 024301.
[32] S. Lalkovski, et al., Phys. Rev. C 87 (2013) 034308.
[33] G. Lorusso, et al., Phys. Rev. Lett. 114 (2015) 192501.
[34] H. Watanabe, et al., Phys. Rev. Lett. 111 (2013) 152501.
[35] https://geant4.web.cern.ch/.
[36] H. Watanabe, Eur. Phys. J. A 55 (2019) 19.
[37] B. Fogelberg, et al., Phys. Rev. C 70 (2004) 034312.
[38] N. Shimizu, et al., Prog. Theor. Exp. Phys. 2021 (2021) 033D01.
[39] J.C. Batchelder, et al., Phys. Rev. C 89 (2014) 054321.
[40] H. Huck, et al., Phys. Rev. C 40 (1989) 1384.
[41] G. Bertsch, et al., Nucl. Phys. A 284 (1977) 399.
[42] T. Otsuka, et al., Phys. Rev. Lett. 123 (2019) 222502.
[43] T. Togashi, et al., Phys. Rev. Lett. 117 (2016) 172502.
[44] C. Yuan, et al., Phys. Lett. B 762 (2016) 237.
[45] I. Towner, Phys. Rep. 155 (1987) 263.
[46] Q. Zhi, et al., Phys. Rev. C 87 (2013) 025803.
[47] J.J. Cuenca-García, et al., Eur. Phys. J. A 34 (2007) 99.
[48] T. Otsuka, et al., Phys. Rev. Lett. 95 (2005) 232502.
[49] K. Schreckenbach, et al., Phys. Lett. B 349 (1995) 427.